Journal of Atmospheric and Terrestrial Physics, Vol. 45, No. 1, pp. 1–14, 1983.
Printed in Great Britain.

0021-9169/83/010001-14 $03.00/0

Field-aligned plasma flow in the quiet, mid-latitude ionosphere deduced from topside soundings

M. LOCKWOOD*
Radio Research Centre, Auckland University, Auckland, New Zealand

(*Received in final form* 10 *May* 1982)

Abstract—A method for quantifying diffusive flows of O^+ ions in the topside ionosphere from satellite soundings is described. A departure from diffusive equilibrium alters the shape of the plasma scale-height profile near the $F2$-peak where ion-neutral frictional drag is large. The effect enables the evaluation of ϕ, the field-aligned flux of O^+ ions relative to the neutral oxygen atom gas, using MSIS model values for the neutral thermospheric densities and temperature. Upward flow values are accurate to within about 10%, the largest sources of error being the MSIS prediction for the concentration of oxygen atoms and the plasma temperature gradient deduced from the sounding. Downward flux values are only determined to within 20%. From 60,000 topside soundings, taken at the minimum and rising phase of the solar cycle, a total of 1098 mean scale-height profiles are identified for which no storm sudden commencement had occurred in the previous 12 days and for which Kp was less than 2o, each mean profile being an average of about six soundings. A statistical study of ϕ deduced from these profiles shows the diurnal cycle of O^+ flow in the quiet, topside ionosphere at mid-latitudes and its seasonal variations. The differences between ϕ and ion flux observations from incoherent scatter radars are considered using the meridional thermospheric winds predicted by a global, three-dimensional model. The mean interhemispheric flow from summer to winter is compared with predictions by a numerical model of the protonospheric coupling of conjugate ionospheres for up to 6 days following a geomagnetic storm. The observed mean (of order 3×10^{16} ions day^{-1} along a flux tube of area 1 m^2 at 1000 km) is larger than predicted for day 6 and the suggested explanation is a decrease in upward flows from the winter, daytime ionosphere between the sixth and twelfth days.

1. INTRODUCTION

It is known that fluxes of plasma along geomagnetic field lines have important consequences for both the ionosphere and protonosphere. By means of such flows the ionosphere is a source of the high density, cold plasma of the plasmasphere which in turn acts as a reservoir, indirectly coupling conjugate F-layers and contributing to their maintenance at night. Although this coupled system has been modelled numerically by various workers (e.g. BAILEY *et al.*, 1978, 1979; MARUBASHI, 1979), relatively few observations of the field-aligned plasma fluxes have been made. Incoherent scatter measurements are restricted to a limited number of locations (VICKREY *et al.*, 1979; EVANS and HOLT, 1978) and roll-modulation of ISIS 2 mass spectrometer data has been used to measure light ion flows at outer plasmaspheric latitudes (FOSTER *et al.*, 1978).

The global morphology of plasma fluxes has mainly been inferred from observations of cold plasma densities. Whistler observations give both the plasma content of a geomagnetic flux tube and the density near the equatorial plane. From the diurnal variations in these quantities at L-values between 3.5 and 5 PARK (1970) deduced daytime flows out of the ionosphere of about 3×10^{12} ions m^{-2} s^{-1} (at 1000 km), with return fluxes at the lower latitudes of roughly half this magnitude on nights of low magnetic activity. This flow pattern for the quiet, inner plasmasphere is confirmed by observations of the polarization rotation and group delay of signals from the ATS 6 geostationary satellite, which yield the total contents of the ionosphere and protonosphere along the slant path (KERSLEY *et al.*, 1978; POULTER *et al.*, 1981). The H^+ density morphology observed by ESRO4 in the topside ionosphere was interpreted in terms of these regions of inflow and outflow by RAITT and DORLING (1976) with upward flow at all local times into the outer plasmasphere. The penetration of permanently upward flows to equatorward of the plasmapause field line was also inferred from topside soundings by BANKS and DOUPNIK (1974) and TITHERIDGE (1976a,c), and was observed directly using ISIS 2 observations of light ion velocities (GREBOWSKY *et al.*, 1978; FOSTER *et al.*, 1978).

The quiet-time behaviour is subject to considerable modification during geomagnetic activity. That the plasmasphere is rapidly depleted following a storm sudden commencement has been demonstrated using density data from whistlers (PARK, 1970) and OGO 5

* Present address: Rutherford Appleton Laboratory, Chilton, Didcot, Oxon OX11 0QX, U.K.

(CHEN and GREBOWSKY, 1978) and using total content data from ATS 6 observations (KERSLEY and KLOBUCHAR, 1980). Magnetic flux tubes have much greater volume at higher latitudes, and consequently the time taken to recover to pre-storm plasma densities is considerably larger. Estimates for this time vary; however, a figure of the order of 1 day can be taken to be appropriate to L near 2.5, whereas at $L = 4$ replenishment typically takes 8 days (PARK, 1974). Hence at low latitudes the recovery time is much smaller than the mean interval between storms, and there is a saturated inner plasmasphere. This is generally in a form of equilibrium with the ionosphere, in that the integrated flux over 24 h is close to zero (PARK *et al.*, 1978). The outer plasmasphere is always in a state of post-storm recovery and plasma flows out of the ionosphere at all times of the day (MARUBASHI, 1979).

Recently particle experiments on board ATS 6, GEOS and then ISEE satellites have revealed that the ionospheric plasma found within the plasmasphere is not just cold and isotropic with energies below about 3 eV, as would be expected for adiabatic bulk flow along the magnetic field lines. Warm plasma components of energies 3–30 eV and composition characteristic of ionospheric origin are found with a variety of pitch angle distributions, particularly in the outer plasmasphere (CHAPPELL *et al.*, 1980). The energizing mechanisms are not yet understood, nor are the implications for the ionosphere-plasmasphere coupling fluxes and the various observations of the bulk plasma parameters. The pitch angle distributions of the ions observed by ISEE imply the replenishment flux is larger from the summer than the winter ionosphere (HORWITZ *et al.*, 1981), a feature also noted by VICKREY *et al.* (1979) from incoherent scatter observations.

One theoretical model of plasmaspheric replenishment following a storm depletion leads to the concept of flux tubes 'filling from the top' (see references given by CHAPPELL *et al.*, 1980). Supersonic flows of protons from the ionospheres of both hemispheres meet near the equatorial plane in the initial recovery phase and establish shock fronts between which high density plasma forms. The fronts propagate earthward, replenishing the flux tubes from the top downwards, as indicated by some plasmapause observations (FOSTER *et al.*, 1978). The existence of any interhemispheric plasma flow means that either the interaction of supersonic flows from the opposite hemispheres is not completely effective in preventing flow across the equatorial plane, or that as the replenishment proceeds the flows quickly become subsonic. The coupling of conjugate ionospheres by such interhemispheric flows has been modelled numerically by BAILEY *et al.* (1978).

2. OBSERVATIONS

In a previous paper LOCKWOOD and TITHERIDGE (1982) described a method for the detection of field-aligned O^+ ion fluxes using topside soundings. The shape of the plasma scale-height profile is altered by such flows only at heights near the $F2$-peak, where ion-neutral drag is large. Because the changes in scale height are caused by this frictional drag it was found useful to express the O^+ flux, ϕ, as a fraction of its limiting value due to the ion drag, ϕ_L, and to define ϕ as

$$\phi = N_i(V_{\parallel} - U_{\parallel}), \tag{1}$$

where N_i is the O^+ density and $V_{\parallel}$ and $U_{\parallel}$ are the upward field-aligned velocities of O^+ ions and neutral atoms, respectively. Values of (ϕ/ϕ_L) can then be determined, to within a few per cent, from each experimental sounding using the neutral exospheric temperature from the MSIS empirical model (HEDIN *et al.*, 1977). The deduced values are not very sensitive to errors in the MSIS prediction and were used to study the global morphology of departures from diffusive equilibrium in the topside ionosphere near sunspot minimum.

In this paper the absolute magnitudes of ϕ are also calculated from the topside soundings. This requires further use of MSIS predictions, and hence the deduced value of ϕ is subject to additional errors which are not present in the (ϕ/ϕ_L) case. Since the largest errors arise from the combined use of model predictions with experimental observations, a limitation on the analysis presented here is that greater numbers of samples must be averaged, and hence the morphology of ϕ cannot be studied with as much detail as that of (ϕ/ϕ_L).

2.1. *Calculation of field-aligned flux, ϕ*

A total of 60,000 topside electron-density profiles have been calculated at the Communications Research Centre, Ottawa, from ionograms obtained between 1962 and 1968 by the *Alouette 1* satellite. Consecutive plasma scale-height profiles were corrected for horizontal gradients and averaged in groups of about six to obtain mean field-aligned variations (as described by TITHERIDGE, 1976a). This yielded 10,000 mean experimental profiles $H(h)$, for altitudes above about 400 km. An example is given in Fig. 1(a). The curve H_p is the best-fit diffusive equilibrium model profile produced using the model of TITHERIDGE (1976a). The fit was obtained by varying the plasma temperature, temperature gradient and ion composition inputs to the model. The presence of any vertical H^+ flux is effectively allowed for by the composition adjustment which alters the O^+/H^+ transition height. However, $H_p(h)$ does not include the effects of any O^+ flux. It also

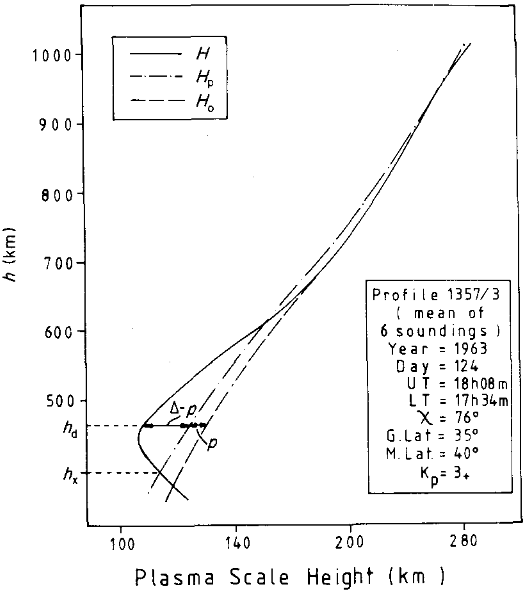

Fig. 1. Example set of plasma scale-height profiles: (a) H is the observed plasma scale-height, (b) H_p is the best-fit, diffusive equilibrium model value and (c) H_o is the true diffusive equilibrium value.

omits F-layer production and loss processes; H_p does not become infinite at the $F2$-peak and it is therefore not fitted to values of H below 400 km.

In most cases the agreement between H and H_p is considerably closer than in Fig. 1. The example does, however, illustrate an effect which is observed in 37% of all cases in that the observed scale height, H, is consistently less than H_p at altitudes just above the $F2$-peak. The decrease occurs in the 400–700 km altitude range and can be modelled by including the effect of field-aligned O^+ flow. This alters the scale-height profile only in the lower topside ionosphere where ion-neutral drag is important. Equation (6) of LOCKWOOD and TITHERIDGE (1982) shows that ϕ, as defined by equation (1), is given by

$$\phi = \frac{N_i}{N_n}\left(\frac{\sin I}{D}\right)\left[m_i g + k\left(\frac{dT_t}{dh}\right)\right]\left[\left(\frac{H_o}{H}\right)-1\right], \quad (2)$$

where N_n is the density of neutral oxygen atoms, m_i the mass of O^+ ions and D the frictional drag coefficient for O^+ ions moving through O atoms; I is the geomagnetic dip; g is the acceleration due to gravity; k is Boltzmann's constant, T_t is the sum of the electron and ion temperatures (T_e and T_i respectively) and H_o is the value of the scale height for diffusive equilibrium conditions. When the concentration of the friction-producing gas, N_n, is large then an upflux of ions ($\phi > 0$) causes H to be less than H_o ($\phi = 0$). At greater altitudes the ionized fraction (N_i/N_n) becomes very large and H approaches H_o independent of the value of ϕ. Equation (2) neglects ion-inertial terms, and the error introduced by this assumption is studied in Appendix B of LOCKWOOD and TITHERIDGE (1982).

The true diffusive equilibrium profile, $H_o(h)$, can also be produced using the model of TITHERIDGE (1976a), by correcting the inputs which generated $H_p(h)$ for the effects of the O^+ flow (LOCKWOOD and TITHERIDGE, 1982). Figure 1 demonstrates that in general H_o differs from H_p. The deviation of H from H_p was scaled off, as in LOCKWOOD and TITHERIDGE (1982), at a height h_d where H_o differs from H by Δ and from H_p by p (as in Fig. 1). In the previous work Δ and p were calibrated for steady-state conditions, enabling the calculation of (ϕ/ϕ_L) from a scaled value for $(\Delta - p)$. These calibrations (see Fig. 2) are used here to evaluate p and this first-order correction applied to H_p to give the value of H_o at the altitude h_d. Magnitudes of (ϕ/ϕ_L) were found to be generally less than 0.5, and Fig. 2 illustrates that for this range p is a small fraction of Δ. By equation (2) the value ϕ is proportional to H_o/H and hence the error introduced by p is small.

The drag coefficient for O^+ ions moving through a neutral atmosphere of O atoms is given by BANKS and HOLZER (1969) to be (MKS units)

$$D = (1.6 \times 10^{-17})m_i \times [T_i + T_n + (4.3 \times 10^{-4})(U-V)^2]^{1/2}. \quad (3)$$

By assuming that at the height h_d the vector difference between the velocities of ions and atoms is field-aligned, equations (1)–(3) can be used to generate a quadratic in ϕ. The relevant root is positive for upward flows and negative for downward ones.

The values of the plasma parameters, N_i, T_t, dT_t/dh, can all be deduced from the experimental sounding (TITHERIDGE, 1976a). The neutral temperature, T_n, and density N_n were taken from the MSIS empirical neutral atmosphere model (HEDIN *et al.*, 1977). The ion temperature, T_i, was deduced using the equation of thermal balance of the ions (ignoring conduction effects) given by BANKS and KOCKARTS (1973)

$$T_i = \frac{T_n + (6 \times 10^6\, N_i/N_T)T_e^{-1/2}}{1 + (6 \times 10^6\, N_i/N_T)T_e^{-3/2}}, \quad (4)$$

where N_T is the total neutral density, also taken from the MSIS model. T_i was iterated to a solution satisfying equation (4) such that

$$T_e + T_i = T_t = H_o\left[\left(\frac{m_i g}{k}\right) + \left(\frac{dT_t}{dh}\right)\right]. \quad (5)$$

Hence ϕ can be calculated from the values of parameters deduced from the plasma sounding and

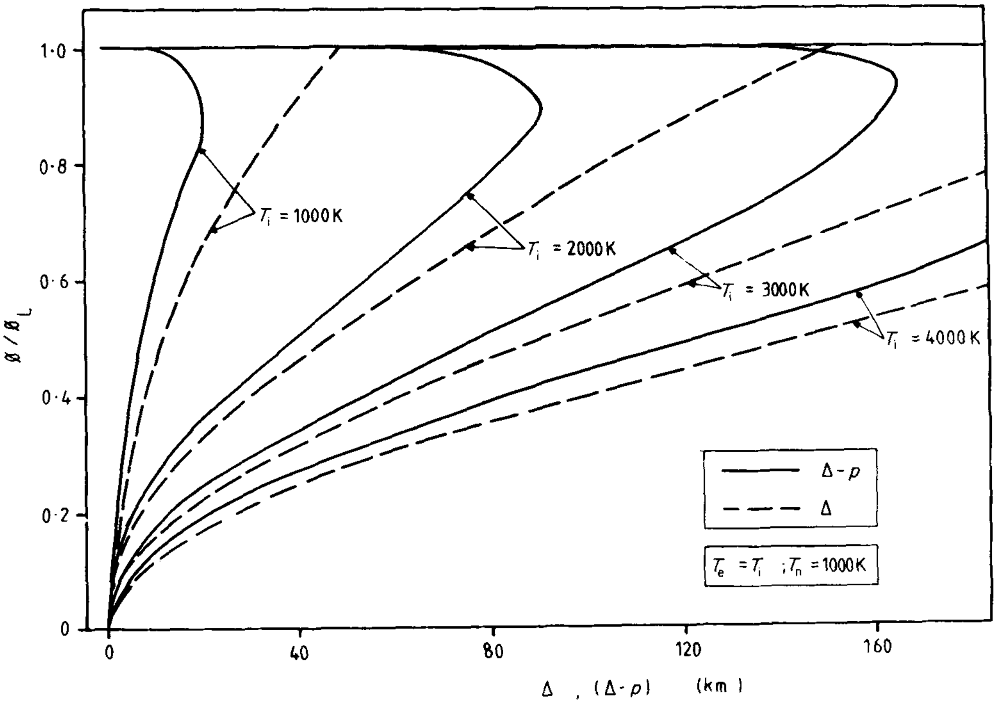

Fig. 2. Calibration curves of Δ and $(\Delta-p)$ as a function of (ϕ/ϕ_L) for plasma temperatures of 1000, 2000, 3000 and 4000 K. The neutral temperature is 1000 K, the plasma temperature gradient is zero, and the electron and ion temperatures are equal.

predicted by the MSIS model, using equations (1)–(5).

During magnetic storms large changes can occur in the composition of the neutral thermosphere, which also cause depletion of the ionospheric plasma. In most cases the only important contribution to the frictional drag on O^+ ions remains that due to neutral O atoms. However, to ensure that other neutral atmospheric gases do not cause any error, a first-order correction to ϕ was applied, calculated by neglecting the term in equation (3) allowing for the velocity difference between O^+ and O, and by assuming that the field-aligned velocities of all neutral constituents are the same. The correction for additional drag, due to molecular oxygen and nitrogen densities of N_{O_2} and N_{N_2}, is then (using the values for the collision frequencies given by Banks and Holzer, 1969)

$$\phi = c\phi' = \phi'\left[1+\left(\frac{6.6N_{N_2}+6.9N_{O_2}}{1.6N_O\sqrt{T_i+T_n}}\right)\right]^{-1}, \quad (6)$$

where ϕ' is the flux value calculated from equations (2) and (3), i.e. by assuming that the drag on O^+ ions is due to O atoms alone. Using the neutral densities predicted by the MSIS model for the values of the $F_{10.7}$ and Ap indices at the time of sounding, the value of c is found to be only slightly reduced from unity on a few winter nights, during the negative phase of a severe magnetic storm.

2.2. *Direction of flow*

The fitting of a model profile, H_p, in the general case when both O^+ and H^+ ions are present, results in a positive value of $(\Delta-p)$ for ϕ of either sense (see Fig. 7 of Lockwood and Titheridge, 1982). For $\phi<0$ the height of h_d (see Fig. 1) is larger than in the corresponding case when $\phi>0$, and this can be used to determine the sense of the field-aligned flow. Titheridge (1976a) deduced the ion transition height, h_T, from the same data set as used in the present study and found values between about 600 and 1400 km at mid-latitudes. From model profiles giving h_T in this range it was seen that h_d was always closer to the $F2$-peak than it was to h_T for upward flows, but never for downward flows. In addition (h_d-h_x) (see Fig. 1) never exceeded 140 km for upward flows. From these two criteria the sense of the detected flow could be determined; the few mid-latitude profiles for which they gave differing results were discarded.

From the model profiles the value of $(\Delta-p)$, for a given magnitude of the O^+ ion flux, was found to be independent of the ion transition height when ϕ is positive but not when it is negative. In principle it is possible to calibrate for this effect, however, interpretation difficulties when $\phi < 0$ (LOCKWOOD and TITHERIDGE, 1982) mean that such a complex correction is not justified. For any given downward flow there is a unique h_T for which $(\Delta - p)$ at $h_d = \Delta$ at h_x (see Fig. 1); this lies in the range 600–800 km which is typical of the ion transition heights deduced by TITHERIDGE (1976a) for the profiles in this database for which $\phi < 0$. If this value for the ion transition height is assumed, H_o at the height h_x can be estimated and ϕ evaluated using the same procedure as is used for upward flows. The error in negative ϕ values introduced by this assumption is discussed in the following section.

2.3. *Accuracy of flux values*

Neglecting the small correction term in equation (3), for the velocity difference between oxygen ions and neutral atoms, equations (2) and (3) give a first-order approximation for ϕ. The first derivatives of this yield estimates of the errors in the flux (due to uncertainties in N_i, N_n, H_o, H, T_i, T_n and $\mathrm{d}T_t/\mathrm{d}h$), maxima of which are shown in Fig. 3, as a percentage of ϕ.

The plasma temperature gradient is determined from the sounding with an accuracy of 20% or ± 0.1 K km^{-1}, whichever is the larger (TITHERIDGE, 1976b). The error in ϕ caused by this uncertainty, α_g, varies with $(\mathrm{d}T_t/\mathrm{d}h)$ as shown in Fig. 3(a). The errors due to the observed and diffusive-equilibrium scale heights, α_f and α_0, depend on $(\mathrm{d}T_t/\mathrm{d}h)$ and the ratio (H_o/H). These are plotted as a function of $|\phi/\phi_L|$ in Fig. 3(b) for the case of upward flows with $(\mathrm{d}T_t/\mathrm{d}h)$ of 0.4 and 8.0 K km^{-1}. This range covers over 95% of the plasma temperature gradient values observed from this data set by TITHERIDGE (1976b). For the lower temperature gradient α_g is smaller than the errors due to the scale heights, however, for the larger value it is greater for the range $|\phi/\phi_L|$ which is observed (LOCKWOOD and TITHERIDGE, 1982).

Also shown in Fig. 3 are estimates of the maximum errors due to the predicted neutral temperature and density, the observed plasma density, and the ion temperature derived using equations (4) and (5) (α_t, α_n, α_p and α_i, respectively). These values are combined into the total error in ϕ shown in Fig. 4 as a function of $(\mathrm{d}T_t/\mathrm{d}h)$ for $|\phi/\phi_L| = 0.1$ and 0.8. The error can be seen to be slightly larger for larger $|\phi/\phi_L|$, however, over the observed range of about 0–0.5, values are approximately constant. At low temperature gradients the error due to the neutral density prediction dominates. For $(\mathrm{d}T_t/\mathrm{d}h)$ exceeding 6 K km^{-1} the error in this gradient becomes the greater but this is only the case in a small fraction of the observations. Overall, individual positive values of ϕ can be taken as being accurate to within 10%, the most important sources of error being the use of the MSIS neutral density prediction and the deduced plasma temperature gradient, in that order.

The values of the ion transition height, h_T, at mid-latitudes during periods of downward flow (as deduced by TITHERIDGE, 1976a) vary between approximately 600 and 800 km, this causes an additional error

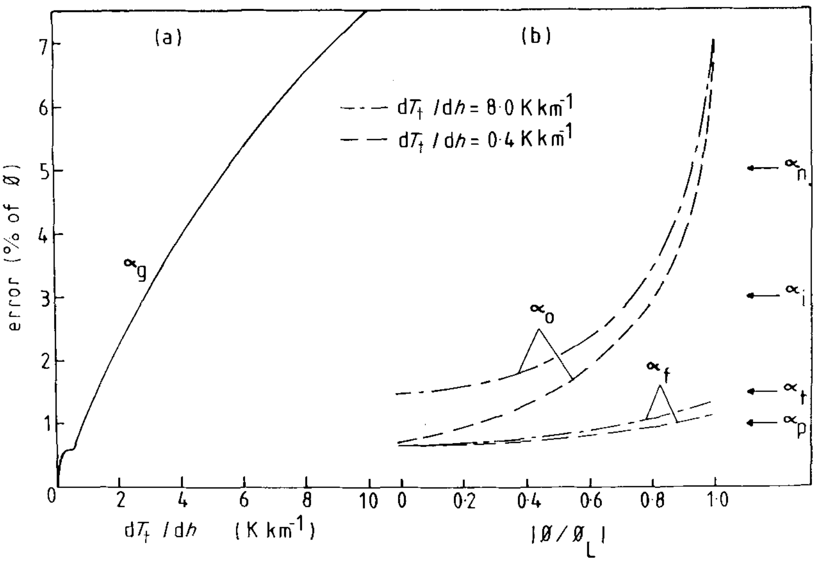

Fig. 3. Maximum errors in upward flux values, as a percentage of ϕ: (a) due to deduced plasma temperature gradient, α_g; (b) due to the scale heights H_o and H, α_0 and α_f, for $(\mathrm{d}T_t/\mathrm{d}h) = 0.4$ and 8.0 K km^{-1}. On the right are shown maxima of the errors α_n, α_i, α_t and α_p due to uncertainties in N_n, T_i, T_n and N_i, respectively.

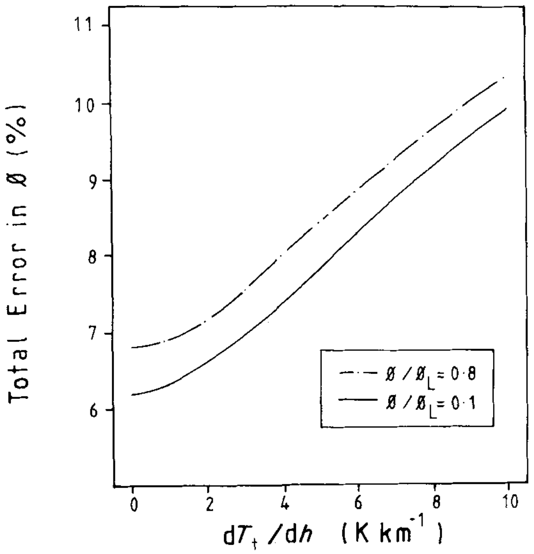

Fig. 4. Total error in each positive value of ϕ as a function of temperature gradient for $|\phi/\phi_L| = 0.1$ and 0.8.

in H_o, and hence ϕ, of up to about 20% for the range $0 > \phi/\phi_L > -0.7$. Hence α_0 is the major error in negative values of ϕ, which can only be regarded as being accurate to within about 20%.

The equations used to calculate ϕ from H and H_o do not assume steady-state; however, the correction applied to H_p to obtain H_o is based on model profiles obtained for steady-state conditions. Hence large departures from steady-state could be responsible for some additional error in the value of ϕ, which is unknown. In addition it is assumed that the H^+ density is sufficiently low to make the contribution to the total field-aligned flux by H^+ ions negligible, even if they have large velocities. In nearly all cases h_T exceeds h_d (for upward flows) or h_x (for downward flows) by an amount sufficient to make this error in the total flux less than 10% for H^+ velocities which are an order of magnitude larger than the O^+ velocities.

2.4. *Analysis*

The database of 60,000 profiles was used to investigate the diurnal variation of field-aligned O^+ ion fluxes in the mid-latitude, topside ionosphere under quiet geomagnetic conditions. Successive soundings were averaged together in groups of about six, as in LOCKWOOD and TITHERIDGE (1982). All storm sudden commencements (SSCs) during the period of observation (1962–1968) were identified and those for which the Kp index subsequently exceeded 4+ in the proceeding 24 h were selected. For each mean profile D_a, the number of whole days (including the one on which it was observed) since a selected SSC, was evaluated.

From his study of whistler data PARK (1974) found that the time taken to replenish the protonosphere following a geomagnetic storm varied from about 1 day at $L = 2.5$ to 8 days at $L = 4$. Theoretical modelling of the plasma flow by MURPHY *et al.* (1976) showed a net flux from the ionosphere to the plasmasphere which persisted for 8 days following the SSC at $L = 3$ for sunspot minimum. This is considerably longer than the period of about 3 days taken for a magnetic flux tube of about this L to recover to its pre-storm total content, as observed by Park. KERSLEY and KLOBUCHAR (1980) found that the total protonosphere content along a slant path to the ATS 6 geostationary beacon satellite took up to 14 days to recover fully. This path covers a range of L; however, the total content measured is applicable to the lower values (POULTER *et al.*, 1981). The study presented here is restricted to observations made at latitudes below 55° (geomagnetic) at which the ionosphere should have largely re-established equilibrium with the protonosphere (in the diurnal sense, in that the daily integrated flux between them is zero) within 12 days of a storm depletion. Magnetically quiet conditions are defined here as when

$$Kp < 2o \text{ and } D_a > 12.$$

This gives sufficient observations to allow a study of quiet-time O^+ fluxes, yet contamination by storm effects is minimized. The total number of mean profiles available in the 30° to 55° and −30° to −55° geomagnetic latitude ranges under these conditions is 1098.

3. RESULTS

Mean values of ϕ and ϕ/ϕ_L are given here for the 30°–55° geomagnetic latitude ranges of both hemispheres and are labelled summer, winter and equinox for all observations taken within 50 days of the summer and winter solstices and the equinoxes, respectively. Profiles showing no departure from diffusive equilibrium are included in the mean values, with ϕ set equal to zero. Only the means of in excess of 20 samples are given. Error bars are plus and minus one standard error, indicating the spread of values about each mean; they do not contain the measurement uncertainties discussed in Section 2.3. All flux values are normalized to the 1000 km level by assuming a dipolar geomagnetic field.

3.1. *Quiet diurnal variations*

Figure 5 shows mean values of ϕ in 2 h LT bins for summer, winter and equinox data from both

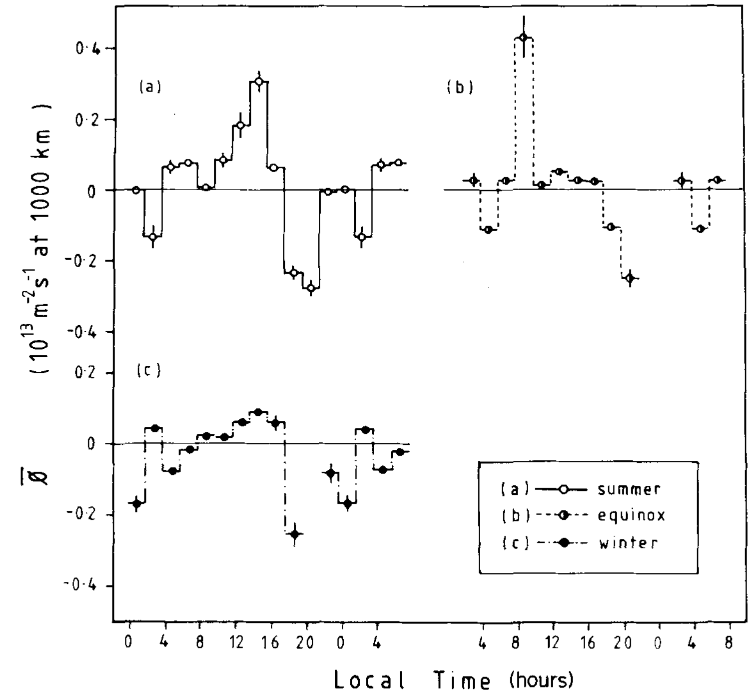

Fig. 5. Mean values of ϕ as a function of local time in 2-h bins for geomagnetic latitudes $\pm(30°–55°)$, $Kp < 2o$ and $D_a > 12$.

hemispheres for which $Kp < 2o$ and $D_a > 12$. The general pattern of quiet-time, mid-latitude O^+ flows observed by incoherent scatter radars (VICKREY *et al.*, 1979; EVANS, 1975) is reflected in the mean values of ϕ with upward flows during the day and downward flows mainly before local midnight. The differences between the observations of ϕ presented here and those of ion flux by incoherent scatter will be discussed in Section 4.1.

For all seasons large downward ion flow, relative to the neutral gas, occurs between sunset and local midnight with peak magnitudes of about

$$0.3 \times 10^{13}\ m^{-2}\ s^{-1}.$$

The largest positive values of $\bar{\phi}$ (upward) are of the order of $0.4 \times 10^{13}\ m^{-2}\ s^{-1}$ and occur following sunrise at equinox and in the afternoon in summer; in winter $\bar{\phi}$ never exceeds $+0.1 \times 10^{13}\ m^{-2}\ s^{-1}$.

The departures from diffusive equilibrium which give the above diffusive flows are demonstrated by Fig. 6. For all seasons the large downward flow before midnight gives large values of $|\phi/\phi_L|$, equal to about 0.25. Hence at these local times the limit set on the O^+ flow by frictional drag is of the order of

$$1.2 \times 10^{13}\ m^{-2}\ s^{-1}$$

and has relatively little seasonal variation. Before sunset larger O^+ flows are achieved with smaller departures from diffusive equilibrium, particularly in summer; this is due to the high plasma density at these times. For all seasons the mean of $|\phi/\phi_L|$ is a minimum following sunrise, indicating that the rise in ϕ due to the onset of solar heating and photo-ionization is smaller than that in ϕ_L. The seasonal variation of ϕ near noon is small but that in $|\phi/\phi_L|$ is large. Together these observations require that ϕ_L be sharply depressed for a few hours around noon in summer, with a minimum value of about $0.5 \times 10^{13}\ m^{-2}\ s^{-1}$. At these times minima in total content and *foF*2 are observed, and from the equation given by TITHERIDGE (1973) this midday biteout should reduce ϕ_L.

3.2. *Integrated ion flow on quiet days*

The diurnal variations of $\bar{\phi}$ shown in Fig. 5 give evidence of a net diffusion of plasma in a day. For example in winter $\bar{\phi}$ is positive after 08 h LT and before 18 h and then again briefly between 02 and 04, the integrated value of the mean flux, I_ϕ, during these periods is 2.3×10^{16} ions m^{-2} and the integrated value of the standard errors in the means, I_σ, is 0.2×10^{16} m^{-2}. The corresponding values for the remainder of the night are -4.5×10^{16} m^{-2} and 0.8×10^{16} m^{-2} respectively, indicating a net mean diffusive flow of -2.2×10^{16} ions m^{-2} day^{-1}. The integrated value of

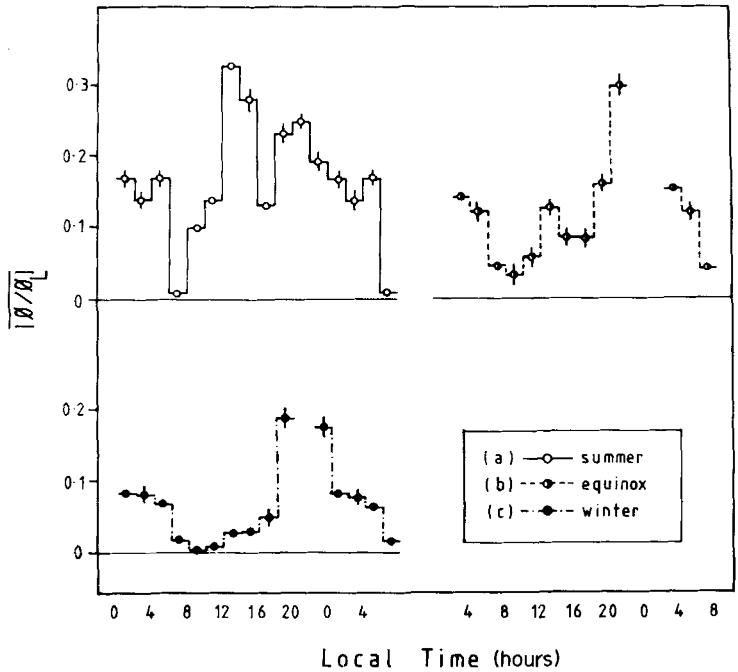

Fig. 6. Mean values of $|\phi/\phi_L|$ as a function of local time in 2-h bins for geomagnetic latitudes $\pm(30°–55°)$, $Kp < 2o$ and $D_a > 12$.

the standard errors for the whole day is $1.0 \times 10^{16}\,m^{-2}$, showing a large spread in the data, but that the net downward diffusion is significant. These values and the equivalent values for summer and equinox are summarized in Table 1. The data for summer suggest a net upward diffusion, with a large statistical spread in the data and for equinox no total flow of significance is observed.

The effects of the measurement errors in each value for ϕ on the values of I_ϕ given in Table 1 are estimated by assuming each positive value of ϕ is subject to the maximum empirical uncertainty of 10% and each negative value has the maximum error of 20%. The resultant errors in I_ϕ, ξ, are also given in Table 1. In every case the effect of measurement errors is less than the statistical spread of the data.

4. DISCUSSION

4.1. *Quiet-time diurnal variations*

By definition, ϕ is the O^+ flux due to diffusion alone (LOCKWOOD and TITHERIDGE, 1982). Thermospheric winds do not affect ϕ directly by momentum transfer to the ions, but only indirectly via redistribution of the plasma and the subsequent diffusive flow. No previous observations of ϕ at mid-latitudes have been reported, but it is constructive to compare the results presented in

Table 1. Integrated mean values of ϕ, I_ϕ; experimental error in I_ϕ, ξ; and the integrated standard error, I_σ (all in units of $10^{16}\,m^{-2}$ at 1000 km)

		Local times	I_ϕ	ξ	I_σ
	Summer	04–18; 00–02	5.9	0.3	1.1
$\bar{\phi} > 0$	Winter	02–04; 08–18	2.3	0.1	0.2
	Equinox	02–04; 06–18	4.5	0.3	0.7
	Summer	02–04; 18–24	−4.6	0.3	0.4
$\bar{\phi} < 0$	Winter	04–08; 18–02	−4.5	0.5	0.8
	Equinox	04–06; 18–02	−4.2	0.5	0.7
	Summer	00–24	1.3	0.4	1.5
Total	Winter	00–24	−2.2	0.5	1.0
	Equinox	00–24	0.3	0.6	1.4

the previous section with observations of field-aligned flow made using incoherent scatter techniques. The latter yields the product $(N_i V_{\parallel})$ which can also be calculated from ϕ by subtracting the product $(N_i U_{\parallel})$ [equation (1)]. Only N_i and not $U_{\parallel}$ is available from the soundings. However, an order of magnitude was calculated for each ϕ value using the meridional component of the thermospheric wind predicted by the global, three-dimensional model of FULLER-ROWELL and REES (1980). The wind predictions used here are for steady-state conditions and allow for the effects of solar EUV heating (for a single value of $F_{10.7}$) and of Joule heating for a model high-latitude convection electric field. The prediction for a solstice or equinox is used for every day in the 100-day periods analysed.

The diurnal variations of the mean values of $(N_i V_{\parallel})$ obtained in this way are shown in Fig. 7. The solid curves give the variations $\bar{\phi}$ for comparison. The difference between the two is usually a small fraction of $\bar{\phi}$, i.e. although h_d varies it is always sufficiently large to ensure N_i and the difference term $(N_i U_{\parallel})$ are comparatively small.

During the day ion flows are upward and the thermospheric winds are generally poleward, hence $U_{\parallel}$ and $V_{\parallel}$ have opposite senses and by equation (1) ϕ exceeds $N_i V_{\parallel}$. Likewise at night the winds are generally equatorward, with greater velocities due to the reduction in ion drag, and the ion diffusion may be downward. At such times ϕ is again smaller in magnitude than $N_i V_{\parallel}$ and both are negative. Owing to the phase lag of the diurnal variation of the winds with respect to sunrise and sunset, there are also times when ions and neutrals have field-aligned velocity components in the same direction. In particular this causes $|\phi|$ to be less than $|N_i V_{\parallel}|$ following summer sunrise and winter sunset.

Although the values of $N_i V_{\parallel}$ have unknown uncertainties due to the application of the model wind values, Fig. 7 does give some understanding as to how ϕ compares with the ion flux that would be observed by a co-located incoherent scatter radar. Figures 8 and 9 show published observations from two such radars. Solstice observations of the vertical O^+ flux at Millstone Hill (after EVANS, 1975) are shown in Fig. 8(a) and the field-aligned flow at Arecibo (after VICKREY *et al.*, 1979) in Fig. 8(b). These two radars are at invariant latitudes of 56° and 32° respectively, and are near the edges of the latitude range studied here. The observations are made at 650 and 544 km and all fluxes are normalized to 1000 km by assuming a dipolar magnetic field. For the magnetic dip at Millstone Hill and observed magnitudes for east–west electric fields and plasma densities the vertical fluxes represent field-aligned values to within 0.1×10^{13} m^{-2} s^{-1}. For

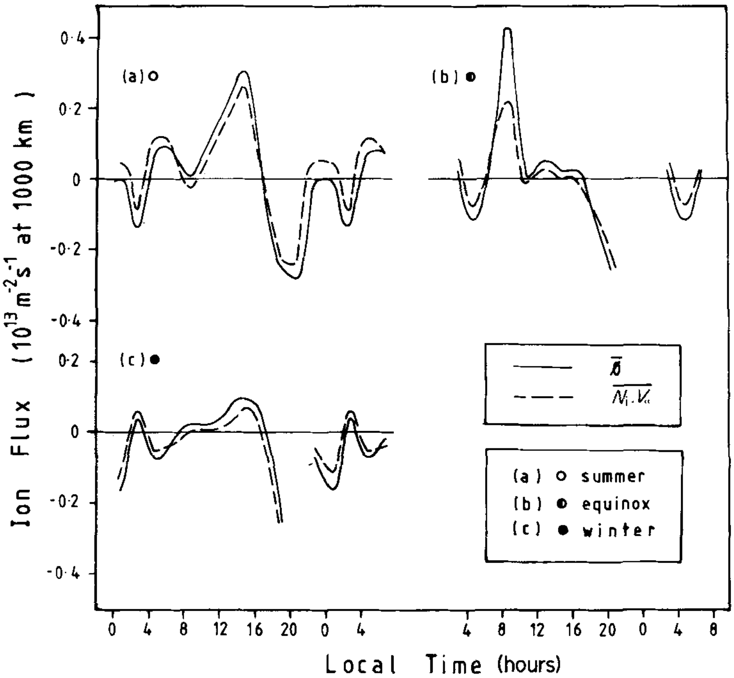

Fig. 7. Variations of the means of $(N_i V_{\parallel})$ and ϕ as a function of local time in 2-h bins for geomagnetic latitudes $\pm(30°–55°)$, $Kp < 2o$ and $D_a > 12$. The product $(N_i V_{\parallel})$ is inferred from the topside soundings using model values for the meridional thermospheric wind.

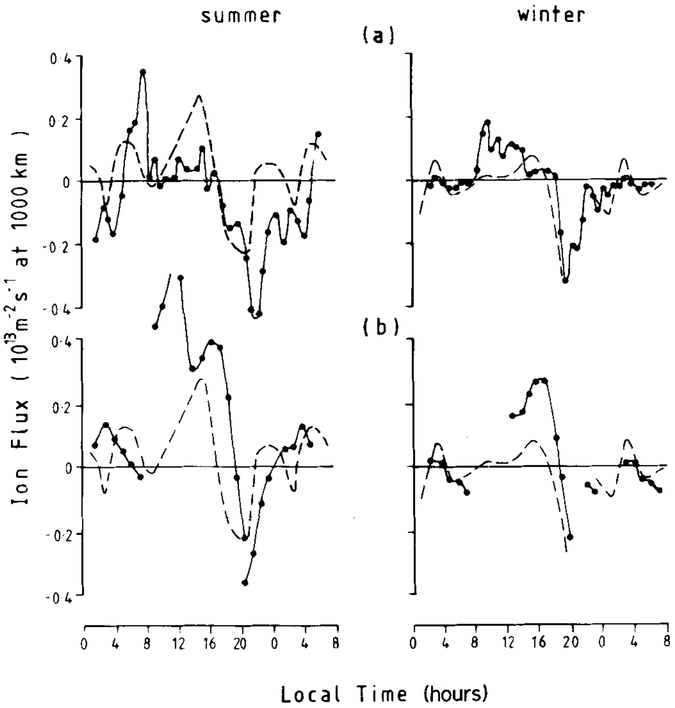

Fig. 8. Diurnal variations of O^+ fluxes for (left) summer and (right) winter: (a) vertical O^+ flux observed at Millstone Hill on 9–10 July 1969 ($\bar{K}p = 2-$) and 20–21 November 1979 ($\bar{K}p = 1-$) (after EVANS, 1975); (b) field-aligned flux at Arecibo on 15–16 August 1976 ($\bar{K}p = 1-$) and 15–16 January 1977 ($Kp = 3o$) (after VICKREY *et al.*, 1979). The dashed curves reproduce the variation of mean $(N_i V_{\parallel})$, given by Fig. 7, for comparison. All flux values are normalized to the 1000 km level.

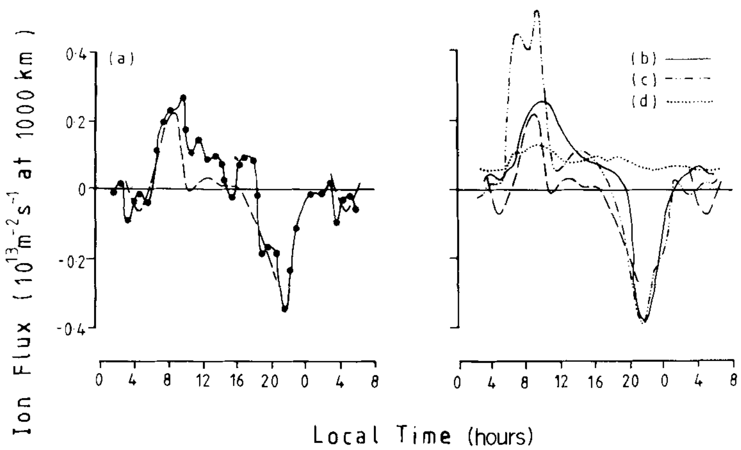

Fig. 9. Diurnal variations in ion fluxes for equinox: (a) vertical O^+ flow observed on 23–24 April 1969 ($\bar{K}p = 2-$) at Millstone Hill (after EVANS, 1975); (b) proton flux at 1000 km modelled for $L = 3$, $D_a = 8$ and sunspot minimum by MURPHY *et al.* (1976); (c) O^+ flux at 600 km and (d) effective H^+ flux at 1000 km modelled for $L = 3$, $D_a = 6$ and sunspot maximum by BAILEY *et al.* (1979). The dashed curves reproduce the variation of mean $(N_i V_{\parallel})$ given by Fig. 7. All flux values are normalized to the 1000 km level.

westward electric fields the given fluxes are larger than the field-aligned value and for eastward electric fields they are smaller.

Although the general diurnal pattern of flow for the three sets of observations are similar there are also considerable differences. The values of $N_i V_{\|}$ deduced from the sounding and the thermospheric models are generally smaller than the flows observed at Arecibo. This is consistent with the increase of $\bar{\phi}$ with latitude across the 30°–55° range (the effects of which can be seen in the results of LOCKWOOD and TITHERIDGE, 1982). However, before noon in summer the difference is very large. The means should also be slightly larger than the field-aligned flow at Millstone Hill but Fig. 8(a) indicates that this may only be true in the afternoon. The Millstone Hill results also show large vertical flows for about 3 h following sunrise for both summer and winter, and these peaks are not reproduced in the means of $(N_i V_{\|})$. The averaging over 2 h LT bins for 25° of latitude and 100-day periods would cause some smoothing of these peaks. Additional differences may be due to east–west electric fields.

Figure 9(a) compares the diurnal variation of mean $(N_i V_{\|})$ with an example equinox day observed at Millstone Hill (after EVANS, 1975; VICKREY *et al.*, 1979 give no equinox results from Arecibo). Agreement near sunrise is much closer than for the solstice results but poorer for all subsequent daylight hours. The right hand side of Fig. 9 compares the mean values of $(N_i V_{\|})$ for equinox with various diurnal variations of ion flux modelled by BAILEY *et al.* (1979) and MURPHY *et al.* (1976) for sunspot maximum and minimum, respectively. Sunspot maximum conditions are only of limited relevance to the data set employed here, however, for this case the authors quote results for the O^+ flux variation on day 6 following a magnetic storm, which are shown in Fig. 9(c). Figure 9(d) shows the effective proton flow into the protonosphere at the times of the O^+ fluxes given in Fig. 9(c); it can be seen that the O^+ flow does not give a good indication of the effective flow into the protonosphere. Electric fields giving cross-L drifts cause additional differences between the two flows (MURPHY *et al.*, 1980). For example when the drift is equatorward (after local midday) tubes of higher total content drift through a given L-value and an apparent large upward flow into the protonosphere is deduced from the rise in total content at that L. However, the H^+ gas at low altitudes is compressed by the drift and for quiet conditions (many days after a storm) this is sufficient to force H^+ down the field lines. This in turn indirectly affects the field-aligned O^+ flow via the charge exchange reaction. After midnight the drift is poleward and the converse of each process occurs.

Figure 9(b) gives the model field-aligned proton flow at 1000 km for sunspot minimum conditions on day 6 following a storm. Complete recovery from the protonospheric depletion is nearly achieved by this day as the characteristic time for replenishment is smaller for sunspot minimum than for sunspot maximum. If steady-state conditions applied to all local times the proton flux at any height h_p, which is well within the protonosphere (such that the O^+ ion density there is negligible) would always equal the O^+ flux at h_d (where the proton density is assumed negligible) with suitable allowance for the divergence of the geomagnetic field lines (EVANS and HOLT, 1978). Generally, however, the O^+ flow is a poor indicator of the simultaneous proton flow at h_p (see references given in LOCKWOOD and TITHERIDGE, 1982).

4.2. *Integrated ion flow in a whole day*

If recovery from the preceding storm depletion could be fully achieved the ionosphere and protonosphere would be in equilibrium in a diurnal sense, in that the total integrated flux between them in both hemispheres is zero in a whole day. In this event the protonosphere between h_p in opposite hemispheres, as well as both topside ionospheres between h_p and h_d, would show no nett growth or depletion in a whole day and the total O^+ flow at h_d would equal the total H^+ flow at h_p, when integrated over a whole day. Considering an h_p equal to the height of the intersection of the flux tube and the equatorial plane shows that under such conditions the total O^+ flow also equals the net interhemispheric flux.

The models of MURPHY *et al.* (1976), (1980) and BAILEY *et al.* (1979) simulate equinox conditions by imposing a boundary condition of zero flux at the equatorial plane and for solstice the flow out of one hemisphere must equal that into the other. Inspection of Table 1 indicates that although no significant value of I_ϕ is found for equinox, the magnitude of the positive I_ϕ value for summer does not equal that of the negative value for winter. Hence although there is some evidence of a flow from the summer to the winter hemisphere, the data do not appear to be consistent. However, for Table 1 the effects of neutral winds have not been included. Table 2 gives the values of I_i, the integrated value of the means of $(N_i V_{\|})$ as discussed in the previous section. No errors are quoted for these values as that due to the neutral wind prediction is unknown; however, the small differences shown in Fig. 7 indicate that these are relatively minor. By integrating over a whole day, errors in the amplitudes predicted for the diurnal variation of meridional wind give no error in I_i. If the integrated value of $U_{\|}$ is predicted to better than 30%, the error in I_i, is less than ε in each case and the total uncertainties are still smaller than the statistical spread of the data, as in Table 1. With the correction for $U_{\|}$ the

Table 2. Integrated mean values of $(N_i V_{\parallel})$, I_i (in units of 10^{16} m^{-2} at 1000 km)

		Local times	I_i
	Summer	04–18; 22–02	6.3
$\bar{V}_{\parallel} > 0$	Winter	02–04; 08–18	1.4
	Equinox	02–04; 06–10; 12–14	3.5
	Summer	02–04; 18–22	−3.7
$\bar{V}_{\parallel} < 0$	Winter	04–08; 18–02	−4.2
	Equinox	04–06; 10–12; 14–02	−3.7
	Summer	00–24	2.6
Total	Winter	00–24	−2.8
	Equinox	00–24	−0.2

integrated flux for equinox is still close to zero and the net daily flow out of the summer hemisphere agrees closely with that into the winter hemisphere (compared with the scale of the errors given in Table 1).

The near zero value for equinox conditions is interesting as it sets a limit to the net effect of the various assumptions. Even for $D_a > 12$ there will be a small amount of protonospheric replenishment occurring, either residual from large storms or from small storms not selected in evaluating D_a. Errors may also have arisen from the analysis procedure applied to the topside profiles, from the MSIS predictions, from the thermospheric wind model values, and from an uneven distribution of samples in the north and south hemispheres and about each equinox. The effect on the value of I_i for equinox is 0.2×10^{16} m^{-2}.

Both summer and winter data presented here are consistent with a flow of plasma from the summer to the winter hemisphere of 2.7×10^{16} ions day^{-1} along a flux tube of 1 m^2 cross-sectional area at 1000 km. This value is a form of average for the magnetic latitude range 30°–55° and for a 100-day period about the solstice. As the interhemispheric flow must fall off between the solstice and equinox, the above value applies on days between the two. Assuming a sinusoidal seasonal variation of the interhemisphere flux gives a peak value of 3.1×10^{16} m^{-2} at the solstice itself.

Vickrey *et al.* (1979) have compared the integrated field-aligned ion flux (both O^+ and H^+) through 750 km observed at Arecibo during the summer and winter days shown in Fig. 8(b). The summer data show a net upward flow and the winter data, although incomplete, indicate a downward flow. The magnitude of the implied interhemispheric flux is about the same as the value given in Table 2, although Fig. 8(b) shows the amplitude of the diurnal cycle of flow is approximately twice as large. Observations of the pitch angle distributions of low energy ions within the plasmasphere by ISEE 1 (Horwitz *et al.*, 1981) also reveal plasma flows from the summer to the winter hemisphere. The O^+ fluxes at Millstone Hill observed by Evans and Holt (1978) show that for most of the solar cycle the night-side protonosphere acts as a plasma source for the winter ionosphere while it is replenished by the summer ionosphere. Hence the protonosphere is able to act to aid the maintenance of the nocturnal winter ionosphere without suffering a large depletion, as suggested by Titheridge (1976a) from the morphology of ion transition heights. The effects of interhemispheric flows on the total plasmaspheric content can be seen in the results of Kersley *et al.* (1978). The content of the northern hemisphere increases following sunrise in the conjugate (summer) ionosphere for December and January. Also for the summer hemisphere the daily reduction in total content commences following sunset in the conjugate (winter) ionosphere and before that in the local, summer ionosphere. These two local time periods are two major contributors to the total summer–winter interhemispheric transport in one day.

Bailey *et al.* (1978) have numerically modelled the flow of plasma along a geomagnetic field line between conjugate ionospheres for the solstices at solar minimum. For times between 20 h LT and midnight the flow is found to be upward in summer and downward in winter in agreement with the conclusions of Titheridge (1976a) and Evans and Holt (1978). These results are for up to six days following a magnetic storm for which the protonospheric density in the summer hemisphere never becomes large enough to force plasma to back down into the ionosphere at night. Figure 7 indicates that for the very quiet conditions used here sufficient pressure is produced to push the O^+ downward in the summer night ionosphere, but H^+ may still simultaneously counterstream upward (see references given in Lockwood and Titheridge, 1982).

The results of Bailey *et al.* (1978) indicate that the protonosphere at mid-latitudes acts as a reservoir of plasma, rather than directly coupling conjugate ionospheres as is the case at lower latitudes. Lockwood and Titheridge (1982) have shown that the transition between these two regions is marked by a large increase in departures from diffusive equilibrium in the topside ionosphere. The model predicts that for $L = 3$ the difference in the daily integrated flux of H^+ through 1000 km in the summer and winter hemispheres is 1.95×10^{16} m^{-2} on day 2 following a magnetic storm falling to 1.38×10^{16} m^{-2} by day 6. Much of this difference is due to the difference in replenishment rates from the two ionospheres, the actual flux across the equatorial plane on these two days totalling 0.93×10^{16} and 0.15×10^{16}, respectively for a flux tube of area 1 m^2 at 1000 km. Hence by day 6 the predicted interhemispheric flow in one day has fallen to an order of magnitude lower than the value given in Table 2. The variation of ion fluxes with latitude discussed above may cause some deviation from the model predictions, which apply close to the poleward edge of the range used here, however, the discrepancy appears too large for this to be the only cause. The model was not run to predict for more than 6 days following a storm. By this time the protonospheric plasma pressure is sufficient to give downward H^+ flows in the winter hemisphere both before midnight and again before sunrise. The total interhemispheric flux in one of these first six days is mainly due to the difference between the flows at night and decreases from one day to the next as the rise in protonospheric plasma pressure reduces this difference. For the conditions studied in this paper (more than 12 days after a major storm and for a lower latitude range) the pressure is higher still and the difference between the night-time flows is further reduced. Tables 1 and 2 show that most of the deduced interhemispheric flow arises because of the smaller total for the upward O^+ flow in the winter dayside ionosphere. This suggests that following day 6 the continuing rise of protonospheric plasma pressure causes a reduction of the upward flows in the dayside ionospheres, affecting the winter hemisphere before the summer and causing the total interhemispheric flow to rise again.

5. CONCLUSIONS

Using MSIS model values for neutral thermospheric densities and temperature, the field-aligned diffusive flux of O^+ ions in the topside mid-latitude ionosphere can be determined from satellite soundings. Upward fluxes are accurate to within 10%, downward flows are only determined to within about 20%. Results for very quiet geomagnetic conditions reveal mean upward flows during the day at magnetic latitudes between 30° and 55°, with return flows at night; chiefly before midnight with smaller downward flows prior to sunrise in all seasons. Using model predictions for the meridional component of thermospheric winds, the mean values are found to be generally consistent with incoherent scatter observations, and the major differences can be explained in terms of the spatial and temporal averaging required to give sufficient samples.

The integrated flux in one day can be used to investigate the daily interhemispheric transport of plasma by assuming that the quiet geomagnetic activity criterion adopted ensures that post-storm replenishment of the protonosphere is negligible. No net interhemispheric diffusion of plasma is found under equinox conditions, however, a summer–winter flow is suggested. The observed difference between the total upward diffusion from the summer hemisphere and the total downward diffusion in the conjugate winter ionosphere is explained by model thermospheric winds. Allowance for such winds reduces the difference in the ion flows to zero and the data are consistent with an interhemispheric flux at the solstices of 3×10^{16} ions day^{-1} along a flux tube of area 1 m^2 at 1000 km. This value is an order of magnitude larger than the prediction of a numerical model of the coupling of conjugate ionospheres by the protonosphere during the first six days following a major magnetic storm. The upward flows in the dayside ionospheres may be reduced during any subsequent days, due to the enhanced protonospheric plasma pressure. Interhemispheric flow would then increase as further replenishment is effected if the reduction in the upward daytime flow in the winter hemisphere occurs prior to the equivalent reduction in the summer hemisphere.

Acknowledgements—Initial research for this work was carried out at the Communications Research Centre, Ottawa, by Dr J. E. Titheridge, to whom the author is greatly indebted. He is also grateful to the Auckland University Council for the award of a Postdoctoral Research Fellowship and to Dr H. Rishbeth for his comments on this manuscript.

REFERENCES

Bailey G. J., Moffett R. J. and Murphy J. A.	1978	*Planet. Space Sci.* **26**, 753.
Bailey G. J., Moffett R. J. and Murphy J. A.	1979	*J. atmos. terr. Phys.* **41**, 417.
Banks P. M. and Doupnik J. R.	1974	*Planet. Space Sci.* **22**, 79.
Banks P. M. and Holzer T. E.	1969	*J. geophys. Res.* **74**, 6317.
Banks P. M. and Kockarts G.	1973	*Aeronomy*, Part B. Academic Press, New York.
Chappell C. R., Baugher C. R. and Horwitz J. L.	1980	*Rev. Geophys. Space Phys.* **18**, 853.
Chen A. J. and Grebowsky J. M.	1978	*Planet. Space Sci.* **26**, 661.
Evans J. V.	1975	*Planet. Space Sci.* **23**, 1461.
Evans J. V. and Holt J. M.	1978	*Planet. Space Sci.* **26**, 727.
Foster J. C., Park C. G., Brace L. H., Burrows J. R., Hoffman J. H., Maier E. J. and Whitteker J.H.	1978	*J. geophys. Res.* **83**, 1175.
Fuller-Rowell T. J. and Rees D.	1980	*J. atmos. Sci.* **37**, 2545.
Grebowsky J. M., Hoffman J. H. and Maynard N. C.	1978	*Planet. Space Sci.* **26**, 651.

HEDIN A. E., SALAH J. E., EVANS J. V., REBER C. A., NEWTON G. P., SPENCER N. W., KAYSER D. C., ALCAYDE D., BAUER P., COGGER L. and MCCLURE J. P.	1977	*J. geophys. Res.* **82,** 2139.
HORWITZ J. L., BAUGHER C. R., CHAPPELL C. R., SHELLEY E. G., YOUNG D. T. and ANDERSON R. R.	1981	*J. geophys. Res.* **86,** 9989.
KERSLEY L., HAJEB-HOSSEINIEH H. and EDWARDS K. J.	1978	*Nature* **271,** 427.
KERSLEY L. and KLOBUCHAR J. A.	1980	*Planet. Space Sci.* **28,** 453.
LOCKWOOD M. and TITHERIDGE J. E.	1982	*J. atmos. terr. Phys.* **44,** 425.
MARUBASHI K.	1979	*Planet. Space Sci.* **27,** 603.
MURPHY J. A., BAILEY G. J. and MOFFETT R. J.	1976	*J. atmos. terr. Phys.* **38,** 351.
MURPHY J. A., BAILEY G. J. and MOFFETT R. J.	1980	*J. geophys. Res.* **85,** 1979.
PARK C. G.	1970	*J. geophys. Res.* **75,** 4249.
PARK C. G.	1974	*J. geophys. Res.* **79,** 169.
PARK C. G., CARPENTER D. L. and WIGGIN D. B.	1978	*J. geophys. Res.* **83,** 3137.
POULTER E. M., HARGREAVES J. K., BAILEY G. J. and MOFFETT R. J.	1981	*Planet. Space Sci.* **29,** 1273.
RAITT W. J. and DORLING E. B.	1976	*J. atmos. terr. Phys.* **38,** 1077.
TITHERIDGE J. E.	1973	*Planet. Space Sci.* **21,** 1775.
TITHERIDGE J. E.	1976a	*Planet. Space Sci.* **24,** 229.
TITHERIDGE J. E.	1976b	*Planet. Space Sci.* **24,** 247.
TITHERIDGE J. E.	1976c	*J. geophys. Res.* **81,** 3227.
VICKREY J. F., SWARTZ W. E. and FARLEY D. T.	1979	*J. geophys. Res.* **84,** 7307.